Available online at www.sciencedirect.com
ScienceDirect
Trans. Nonferrous Met. Soc. China 23(2013) 2431−2438
Transactions of Nonferrous Metals Society of China
www.tnmsc.cn

5-methyl-1H-benzotriazole as potential corrosion inhibitor for electrochemical-mechanical planarization of copper

Yan-fei BIAN, Wen-jie ZHAI, Bao-quan ZHU

School of Mechatronics Engineering, Harbin Institute of Technology, Harbin 150001, China

Received 4 July 2012; accepted 18 February 2013

Abstract: According to the electrochemical analysis, the corrosion inhibition efficiency of 5-methyl-1H-benzotriazole (*m*-BTA) is higher than that of benzotrizaole (BTA). The inhibition capability of the *m*-BTA passive film formed in hydroxyethylidenediphosphonic acid (HEDP) electrolyte containing both *m*-BTA and chloride ions is superior to that formed in *m*-BTA-alone electrolyte, even at a high anodic potential. The results of electrical impedance spectroscopy, nano-scratch experiments and energy dispersive analysis of X-ray (EDAX) indicate that the enhancement of *m*-BTA inhibition capability may be due to the increasing thickness of passive film. Furthermore, X-ray photoelectron spectrometry (XPS) analysis indicates that the increase in passive film thickness can be attributed to the incorporation of Cl^- into the *m*-BTA passive film and the formation of $[Cu(I)Cl(m\text{-BTA})]_n$ polymer film on Cu surface. Therefore, the introduction of Cl^- into *m*-BTA-containing HEDP electrolyte is effective to enhance the passivation capability of *m*-BTA passive film, thus extending the operating potential window.
Key words: electrochemical-mechanical planarization; 5-methyl-1H-benzotriazole; corrosion inhibitor; chloride ion

1 Introduction

Chemical-mechanical polishing (CMP) technology has become a widely used technique for planarization removal. Traditional CMP technology faces severe challenges due to the introduction of new porous low-*k* dielectric material, which may be damaged easily in the CMP process. In order to overcome the inherent defects of CMP, electrochemical-mechanical polishing (ECMP) technology has been introduced and gotten more and more attention. Composite of electrolyte is very important which could lead to high removal rate, widely operating potential window and highly surface quality [1−3]. In ECMP electrolyte, benzotriazole (BTA) is a commonly used corrosion inhibitor of Cu by forming a BTA passivation film to promote the planarization efficiency [4,5]. Nevertheless, BTA passive film is only stable at a low operating potential in the HEDP electrolyte, which results in a narrow operating potential window.

STEWART et al [6] reported that the addition of chloride ions (Cl^-) in an acid (about pH=2) solution containing BTA could increase the thickness of the BTA passive film and result in significant reduction of removal rate. They thought that the removal rate decreased because Cl^- was coordinated to Cu−BTA film with Cu(I) center which formed strong and impact passive film [7]. LIN and CHOU [8] found that adding a low concentration of chloride ions into acidic ECMP electrolyte with BTA would increase the BTA passivation film thickness and promote the inhibition capability of BTA.

In this study, the inhibition efficiency of *m*-BTA in HEDP electrolyte was investigated at various anodic potentials. The results show that *m*-BTA can be used as an efficient corrosion inhibitor instead of BTA in ECMP. Due to the insufficient inhibition ability in the HEDP-based electrolyte containing *m*-BTA alone at a high operating potential, the objective is to enhance the inhibition capability and the operating potential window of the *m*-BTA passivation layer at a low pH value by introducing Cl^- into the HEDP-based electrolyte. Various electrochemical measurements including polarization tests, electrochemical impedance spectroscopy (EIS) and nano-scratch tests were used to evaluate and characterize the inhibition efficiency of the *m*-BTA passive film formed in the HEDP electrolyte with or without Cl^- at various anodic potentials. In addition, the nature of the

Foundation item: Project (50975058) supported by the National Natural Science Foundation of China
Corresponding author: Yan-fei BIAN; Tel: +86-451-86413802; E-mail:bianyfchengyy@gmail.com
DOI: 10.1016/S1003-6326(13)62751-X

m-BTA passive film with or without Cl^- was also further investigated by using energy dispersive analysis of X-rays (EDAX) and X-ray photoelectron spectroscopy (XPS).

2 Experimental

All the experiments were carried out on a simulated electrochemical mechanical polishing equipment [9,10]. Wafers were plated using a plating bath consisting of 200 g/L cupric sulfate, 30 mL/L sulfuric acid, 100 mg/L chloride ion, 6 mL/L acid copper making up agent HN−610MU, 0.4 mL/L acid copper brightener HN−610A and 0.4 mL/L acid copper brightener HN−610B (Highnic Group). Samples were typically plated at a rate of 10 mA/cm^2 for approximately 20 min. The basic electrolyte composition in the experiments consisted of 6% HEDP (mass fraction), deionized water and sodium chloride solid. Before each experiment, the wafer sample was polished by using 3000 grit sand paper and 1 μm diamond grit suspension to obtain a mirror finish.

In this study, the electrochemical measurements including potentiodynamic polarization test and EIS were carried out using a computer-controlled electrochemical analyzer, CHI604D (CH Instrument). A copper plate was used as the counter electrode, in addition to a saturated calomel reference electrode (SCE). Voltammetry measurements were made with or without abrasion using samples in an electrochemical mechanical polishing machine. In order to avoid the low-frequency signal drift, a frequency range of 20 Hz−20 kHz was used through appropriate selection of low frequency to generate a quasi-steady-state result.

All EIS studies were performed using a 5 mV amplitude sinusoidal AC voltage signal in the tested frequency range of 20 Hz−20 kHz. The ZSimp Win version 3.1 was used to fit the EIS data by complex nonlinear least square (CNLS) analysis. For each EIS test, the electrode was held for 10 min to form the passive film. TRIPATHI et al [11] claimed that the impedance behavior did not vary significantly no matter whether the electrode rotated or not, hence EIS tests were performed in static condition.

Potentiodynamic polarization test and EIS were used to calculate and characterize the inhibition efficiency of *m*-BTA passivation film formed in HEDP electrolyte with or without chloride ion at various operating voltages. EDAX was used to measure the content of chloride ion on the surface of different wafer samples, which could be expected to obtain the relation between the concentration of chloride ion and the thickness of *m*-BTA passive film. Further nano-scratch tests were performed to obtain the thickness of the *m*-BTA passive film formed in the electrolyte with or without chloride ion. The chemical composition of the surface was determined using XPS. The XPS measurements were conducted by PHI 5700 ESCA system with a monochromatic Al K_α source and a charge neutralizer.

For all wafer polishing experiments, the down force was 1 N, the platen speed was 100 r/min, and the polyurethane pad was used. The pad was perforated with holes of 1 mm in diameter at regular intervals, with an overall pad porosity of approximately 6.20%.

3 Results and discussion

3.1 Electrochemical measurements

The results of the polarization measurements comparing the inhibition efficiency between BTA and *m*-BTA in static condition are shown in Fig. 1. Addition of 0.1% BTA to 6% (mass fraction) HEDP electrolyte can significantly inhibit the Cu dissolution when the voltammetry is less than 0.7 V (vs SCE). While 0.1% *m*-BTA is added to the 6% HEDP electrolyte, the inhibition potential region widens to about 1.0 V (vs SCE). This fact indicates that *m*-BTA is a promising inhibitor instead of BTA.

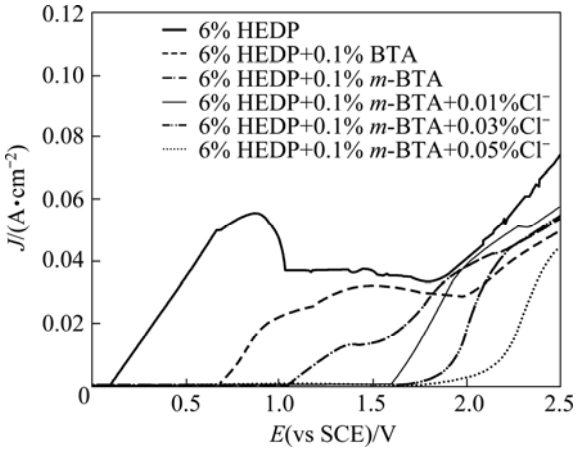

Fig. 1 Static polarization curves performed from 0 to 2.5 V (vs SCE) at scan rate of 5 mV/s in different solutions

The polarization curves with different Cl^- concentrations in HEDP electrolytes without containing the inhibitor *m*-BTA are shown in Fig. 2. When the Cl^- concentration increases, the current density slightly decreases within potential window from 1.0 to 1.7 V (vs SCE). It may be possibly attributed to the formation of a Cl^--containing film on Cu surface in this potential interval. The mechanism of Cu dissolution under external anodic potential in chloride media has been extensively reported by many authors. KEAR et al [12] reported that the formation of $CuCl_2^-$ on Cu surface may be due to the kinetics of anodic dissolution of Cu in

solution in the absence of inhibitor. Obviously, the addition of Cl^- into HEDP-based electrolyte without containing *m*-BTA is ineffective to inhibit Cu dissolution. However, it is interesting to find that, when adding low concentration inhibitor of 0.01% *m*-BTA to HEDP electrolyte containing various concentrations of Cl^-, the inhibition capability of *m*-BTA increases with the Cl^- concentration and the effective inhibition potential also extends from 1.0 to 1.5 V (vs SCE). The above results suggest that the electrolyte can improve the passivation effect and operating potential window by adding Cl^- and *m*-BTA, even at a high anode potential.

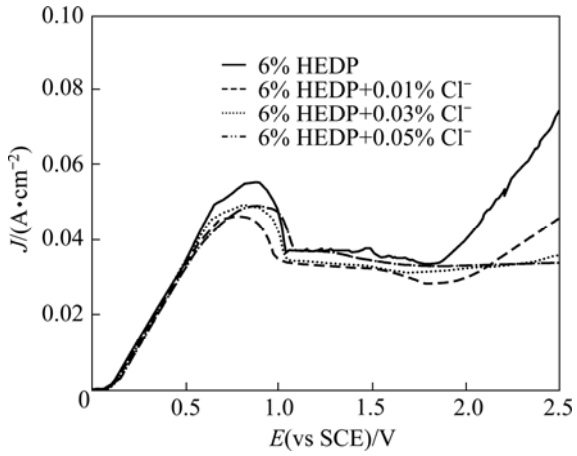

Fig. 2 Static polarization curves performed from 0 to 2.5 V (vs SCE) at scan rate of 5 mV/s in HEDP-based electrolyte containing different Cl^- concentrations

Figure 3 shows the Tafel plots of copper. The corrosion potential increases with the Cl^- concentration, which indicates that Cl^- has a good synergic effect with *m*-BTA in HEDP electrolyte.

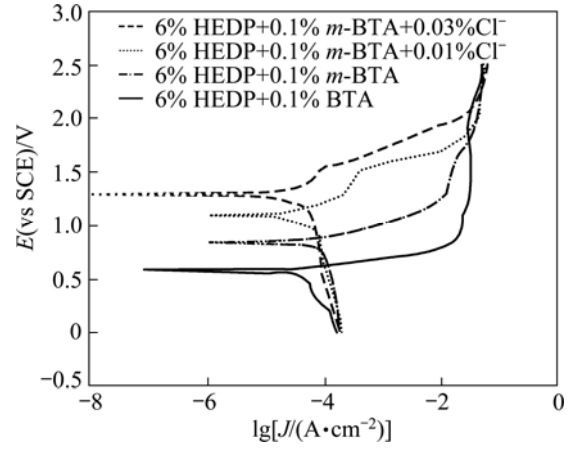

Fig. 3 Potentiodynamic polarization curves of copper under Cl^--containing in the absence and in the presence of *m*-BTA

3.2 Polishing experiments

The potentiodynamic curves in simulated ECMP equipment are shown in Fig. 4. It is demonstrated that the effective operating potentials of BTA passive film and *m*-BTA passive film are about 0.7 and 1.0 V (vs SCE), respectively. It is also shown that the effective operating potentials of *m*-BTA passive film without and with the incorporation of Cl^- are about 1.0 and 1.7 V (vs SCE), respectively. The current density increases with the abrasion, primarily due to the depletion of passive film. The removal rate of copper mainly depends on the applied external current and can be estimated by the Faraday's law. Therefore, a planarization factor is defined as [13−15]

$$\varepsilon_{\mathrm{ECMP}} = \frac{I_{\mathrm{abrasion}} - I_{\mathrm{noabrasion}}}{I_{\mathrm{abrasion}}} \quad (1)$$

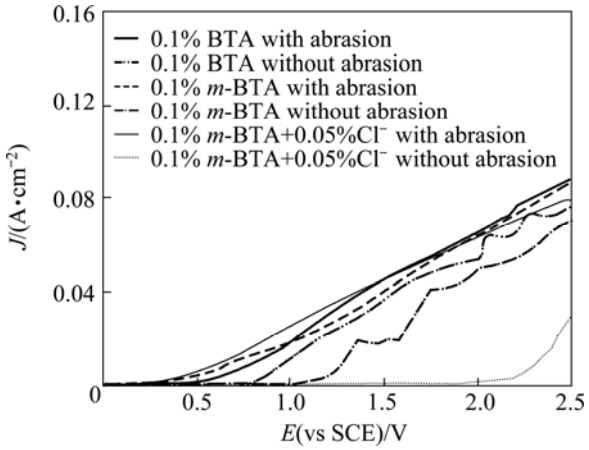

Fig. 4 Potentiodynamic curves of Cu without and with abrasion (Sweep potential was performed from 0 to 2.5 V (vs SCE) at scan rate of 5 mV/s)

It can be seen obviously from Fig. 5 that the planarization efficiency with *m*-BTA is higher than that with BTA within all ranges, which means that the inhibition efficiency of *m*-BTA is superior to that of BTA. Although the planarization efficiency for HEDP electrolyte containing *m*-BTA or BTA reaches up to 0.7, the Cu removal rates are less than 600 nm/min. For HEDP electrolyte containing only *m*-BTA, the planarization factor can only reach 0.50 when the removal rate reaches 600 nm/min at a potential of about 1.3 V (vs SCE). However, for HEDP electrolyte containing *m*-BTA with 0.05% Cl^-, the planarization factor can even reach 0.98 when the removal rate reaches 600 nm/min at a potential of about 1.1 V. Chloride ion shows synergic effect with *m*-BTA in HEDP electrolyte, namely, Cl^- incorporation into HEDP electrolyte can guarantee sufficient Cu removal rate (>600 nm/min) as well as high $\varepsilon_{\mathrm{ECMP}}$ (>0.95).

Under the condition of $\varepsilon_{\mathrm{ECMP}}$>0.7, Cu removal rate greater than or comparable to 600 nm/min (27 mA/cm^2) and surface roughness <16 nm is ideal for a 10 μm scan using AFM [11,15]. These parameters should be taken

into consideration in optimizing the electrolytes. AFM images of copper surface before and after the ECMP process were characterized by means of AFM measurements, as shown in Fig. 6. It can be noted that the surface roughness values before and after ECMP process are 13.9 and 11.5 nm, respectively. These results indicate that the Cl^--containing HEDP electrolyte with *m*-BTA can be used for ECMP process, especially in the case of higher anodic potential.

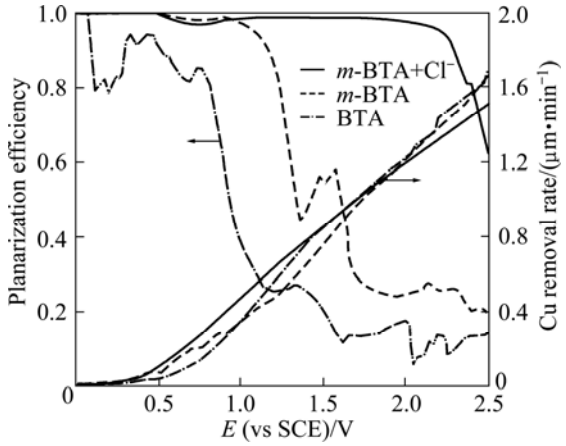

Fig. 5 Cu removal rate and planarization efficiency for ECMP electrolyte containing 0.1% BTA, 0.1% *m*-BTA and 0.1% *m*-BTA and 0.05% Cl^-.

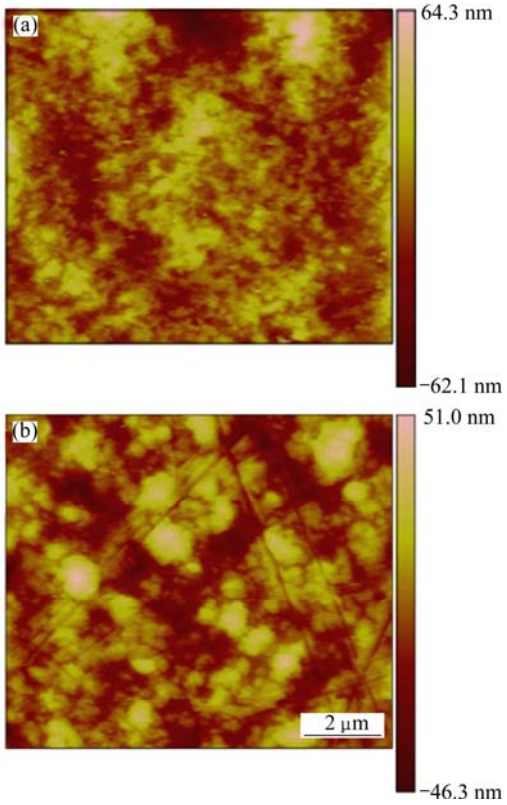

Fig. 6 3D AFM images obtained before (a) and after (b) ECMP process in HEDP electrolyte containing 0.1% *m*-BTA and 0.05% Cl^- at constant applied potential of 1.2 V (vs SCE) for 60 s

3.3 Characterization of passive film

Figure 7 shows the Nyquist plots of impedance studies on ECMP electrolytes containing 0.1% *m*-BTA with or without 0.05% Cl^- at different anodic potentials. The measured impedance parameters are analyzed on the basis of the equivalent circuit model shown in the inset figure of Fig. 7, which consists of four elements, the solution resistance (R_s), the charge-transfer resistance (R_{ct}), the constant phase element (C_{PE}) and the Warburg impedance (W) [16−19].

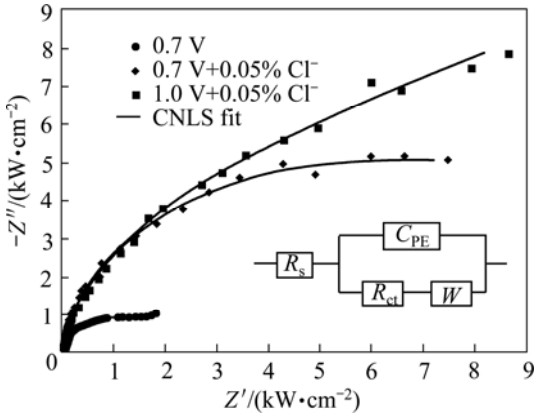

Fig. 7 Nyquist impedance plots for HEDP electrolyte containing 0.1% *m*-BTA with or without 0.05% Cl^- (Inset figure is equivalent circuit model for Cu passive film)

The impedance parameters presented in Table 1 are the best-fit results to the equivalent circuit in Fig. 7, omitting the value W. It can be seen that, when Cl^- is present in HEDP electrolyte, the C_{PE} value decreases and R_{ct} value increases. The increment of R_{ct} implies the formation and growth of Cu. The decrease in the C_{PE} value can be attributed to the gradual replacement of water molecules and other ions originally absorbed on the surface through the adsorption of inhibitor molecules on the metal surface, which may result from a decrease in the local dielectric constant and/or an increase in the double layer thickness [20].

Table 1 Best-fit values for R_s, R_{ct}, C_{PE} and n of equivalent circuit in Fig. 7

Reaction film	Operating potential/V	R_s/ ($\Omega\cdot cm^2$)	R_{ct}/ ($\Omega\cdot cm^2$)	C_{PE}/ ($\mu F\cdot cm^{-2}$)	n
m-BTA	0.7	12.39 (1.63)	1668 (1.41)	9.278 (2.26)	0.9466 (0.249)
Cl^--containing *m*-BTA	0.7	11.76 (4.93)	9076 (2.71)	3.963 (2.69)	0.9514 (0.299)
Cl^--containing *m*-BTA	1.0	10.12 (4.63)	8257 (6.71)	3.160 (4.55)	0.9296 (0.610)

Note: Data in parentheses is fitting error.

Table 2 lists the results of EDAX for the wafer samples which were immersed in the 6% HEDP

electrolyte with or without Cl^- in the range of 0.01% to 0.05% at a constant potential of 0.7 V (vs SCE) for 180 s. The EDX analysis reveals that the passive film consists of Cu, O, Cl, C and N. It is shown that the content of Cl^- measured from passive film increases with the concentration of Cl^- in the electrolyte, suggesting that the enhancement of inhibition capability can be attributed to the incorporation of Cl^- into *m*-BTA passive film.

Table 2 Results of EDAX (mass fraction, %)

Cl^-	C	N	O	Cl	Cu
−	0.22	0.12	5.30	0.18	94.18
0.01	0.26	0.13	6.17	0.20	93.24
0.03	0.30	0.15	6.48	0.23	92.84
0.05	0.63	0.31	6.19	0.48	92.39

Further nano-scratch experiments were used to obtain the thickness of the *m*-BTA passive film formed in the electrolyte with or without chloride ion. A simple model was proposed to estimate the thickness of the reacting layer [21]. The height of pile-up before the indenter and the friction in the interface are omitted during the scratching. The forces acting on the indenter is illustrated in Fig. 8, and it can be expressed as

$$F_n = \frac{\sqrt{3}}{6}\sigma_{ys}w_1^2 + \frac{\sqrt{3}}{6}\sigma_{yf}(w_2^2 - w_1^2) \quad (2)$$

$$F_t = \sigma_{ys}(\frac{1}{2}w_1d_1) + \sigma_{yf}(\frac{1}{2}w_2d_2 - \frac{1}{2}w_1d_1) \quad (3)$$

where w_i is the width of the scratch grooved track as shown in Fig. 8 and $w_i = 2\sqrt{3}d_i\tan\theta$, θ=65.3°; F_n is the normal force; F_t is the tangential force; σ_{yf} is the mean contact pressure of soft layer; σ_{ys} is the substrate mean contact pressure; d_1 and d_2 are the effective penetration depth of substrate and the scratch depth during experiment, respectively. There are two unknown parameters in Eqs. (2) and (3), d_1 and σ_{yf}. The value of the substrate mean contact pressure can be obtained based on the assumption that the film thickness is 0 according to Eqs. (2) and (3). Other parameters can be obtained by the scratch data of wafer samples. The data is listed in Table 3. The thickness of the passive film can be calculated by (d_2-d_1), which are about 1.47 and 3.39 nm without and with Cl^-, respectively. To verify the film thickness measurement from our model, X-ray photo-electron spectroscopy (XPS) was used to estimate the film thickness. Following the method proposed by CHAWLA et al [22], angle resolved XPS was used to model the thickness, structure and composition of the film. The experimental XPS signal intensity ratio is shown in Fig. 9. A two-layer model was used by CHAWLA et al [22]. The first layer was hydroxyl and bound water, and the second layer was cuprite, Cu_2O. In order to follow their method, the same two-layer model was used to calculate the thickness of those two layers. Then it is assumed that the two layers have the same material properties and the overall thickness is compared to the thickness of our single-layer nano-scratch model. To reduce the effect of surface roughness on photo-electron angular distribution, only high angle data (80°) are used to fit the equation. The calculated results are listed in Table 4. From comparison between Tables 3 and 4, the thickness measurements of these two techniques are very close to each other, which confirms the model in this experiment. The results imply that Cl^- may be incorporated into the *m*-BTA passive film, henceforth, addition of Cl^- increases the thickness and inhibition capability of the passive film.

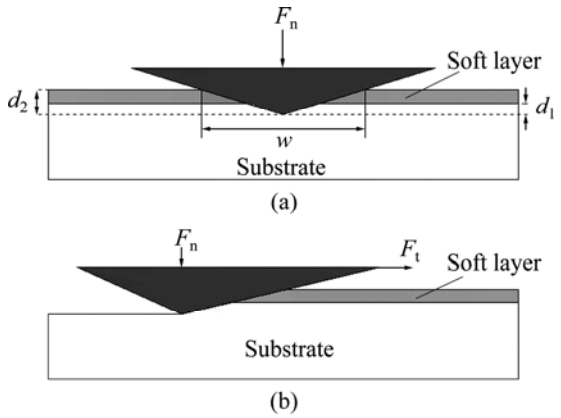

Fig. 8 Schematic of nano-scratch experiment: (a) Front view; (b) Lateval view

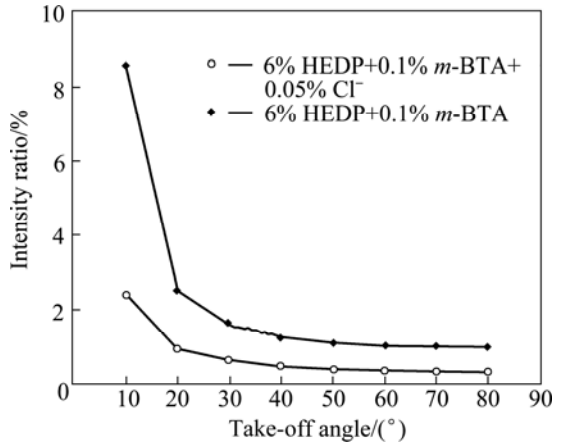

Fig. 9 XPS signal intensity ratio with take-off angle from Cu surface

Table 3 Results of nano-scratch test

Sample	F_n/mN	F_t/mN	d_2/nm	d_1/nm	(d_2-d_1)/nm
Pure copper	0.278	0.064	23.506		
m-BTA	0.278	0.064	29.702	28.234	1.468
Cl^--containing *m*-BTA	0.278	0.064	33.297	29.909	3.388

Table 4 Results of XPS measurement in Fig. 9

Sample	1st layer thickness/nm	2st layer thickness/nm	Over thickness/nm
m-BTA	0.4	0.9	1.3
Cl^--containing *m*-BTA	0.2	3	3.2

Figure 10 shows the XPS spectra of copper under *m*-BTA-containing HEDP electrolyte in the absence and in the presence of Cl^-. Figures 11 and 12 show the XPS spectra of Cu and O(1s) lines with or without Cl^-, respectively. Figure 11 demonstrates that no divalent Cu(II) ions are found on the Cu surface when *m*-BTA is present in HEDP electrolyte, while Fig. 12 demonstrates that $Cu(OH)_2$ peak can be still observed on the Cu surface. DU et al [23] found that no cupric oxide was detected in Cu(2p) XPS spectra, but $Cu(OH)_2$ was observed in O(1s) XPS spectra when Cu was immersed in a potassium biphthalated buffer solution containing 10% H_2O_2, 1% glycine, and 0.125% copper sulfate for 10 min. They suspected that the detection of $Cu(OH)_2$ peak may be due to the adsorption of $(OH)^-$ radicals on Cu surface after Cu electropolishing in phosphate electrolyte. The peak appeared at 532.95 eV is due to the presence of adsorbed H_2O molecules. Furthermore, the Cu-*m*-BTA complex formation on Cu surface is confirmed by N(1s) XPS spectra. Figure 13 shows the N(1s) peak at 399.5 and 399.7 eV obtained in *m*-BTA

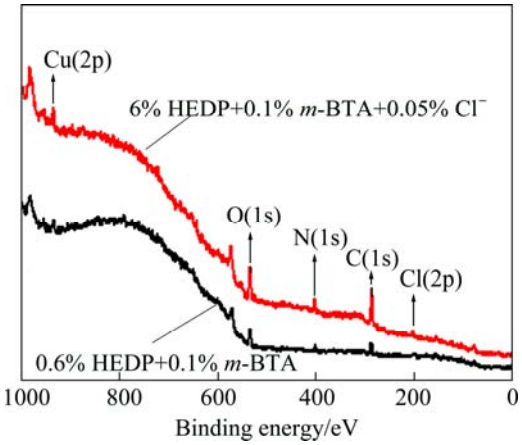

Fig. 10 XPS spectra of copper under *m*-BTA-containing HEDP electrolyte in the absence and presence of Cl^-

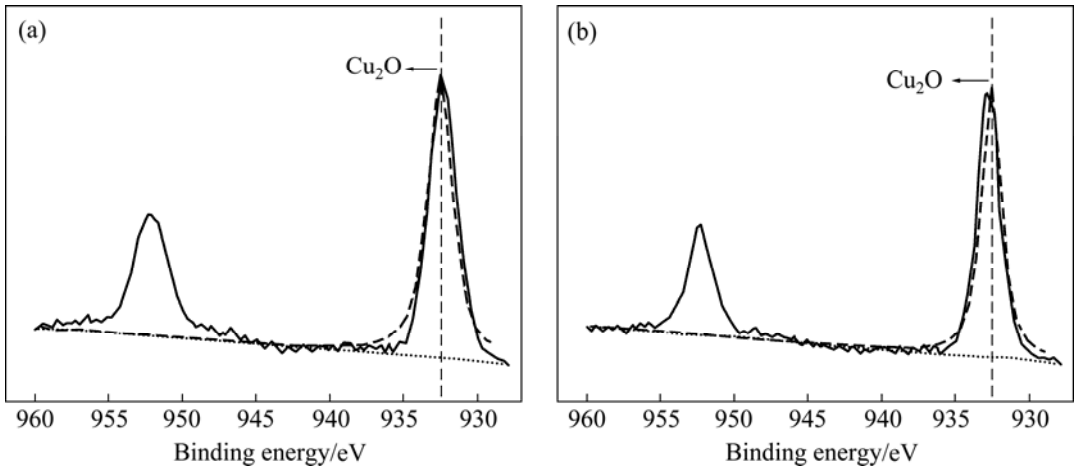

Fig. 11 XPS spectra from surface of Cu film in HEDP-based electrolyte containing 0.1% *m*-BTA (a) and 0.1% *m*-BTA+0.05% Cl^- (b)

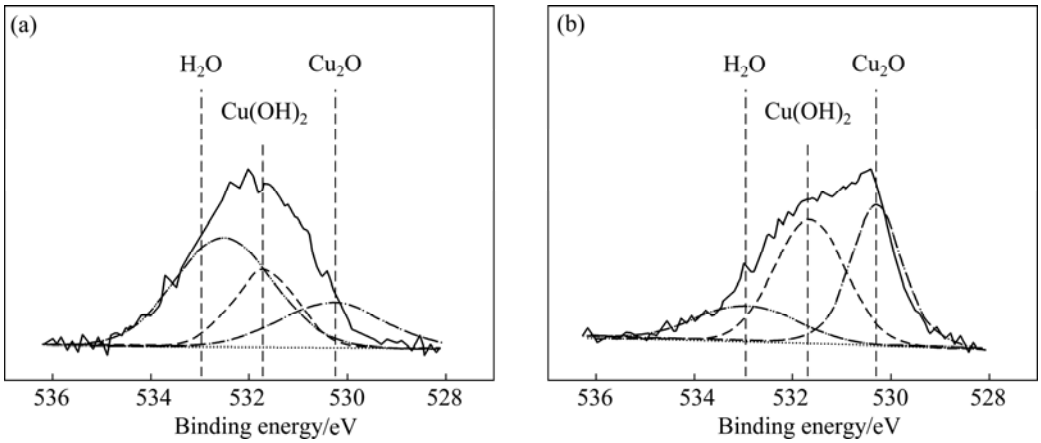

Fig. 12 XPS spectra from Cu surface of O(1s) line in HEDP-based electrolyte containing 0.1% *m*-BTA (a) and 0.1% *m*-BTA + 0.05% Cl^- (b)

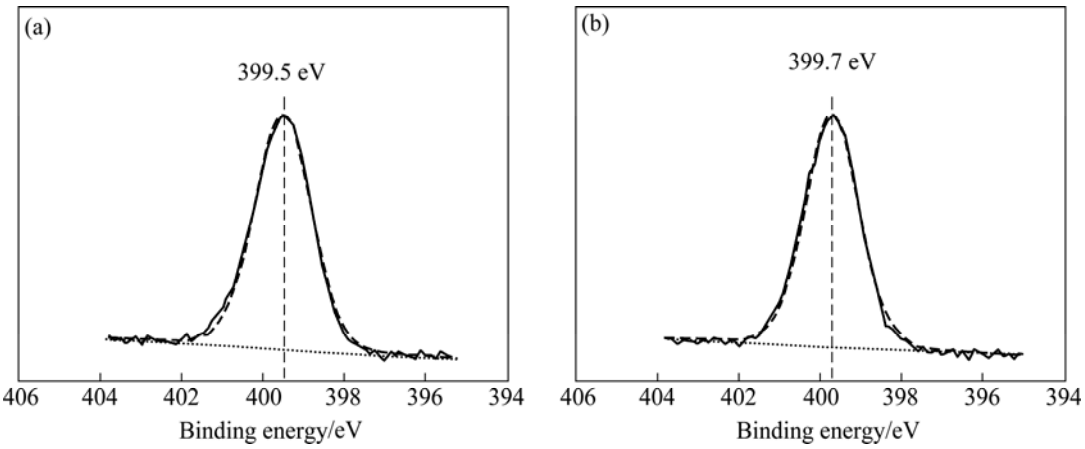

Fig. 13 XPS spectra from Cu surface of N(1s) line in HEDP-based electrolyte containing 0.1% *m*-BTA (a) and 0.1% *m*-BTA + 0.05% Cl^- (b)

containing HEDP electrolyte without and with Cl^- can be attributed to the adsorption of Cu-*m*-BTA complex on the Cu surface, implying that the decrease in Cu dissolution rate may be due to the formation of Cu-*m*-BTA passive film on the Cu surface. Therefore, the passive film formed in HEDP electrolyte both containing *m*-BTA and Cl^- is composed of the atoms of Cu(I), N and Cl^-, and the passive film can be represented as the complex, $[Cu(I)Cl(m\text{-BTA})]_n$. The XPS measurements demonstrate that the enhancement of inhibition capability can be attributed to the incorporation of Cl into *m*-BTA passive film and coordination with the Cu(I) center in the *m*-BTA passive film.

4 Conclusions

1) The inhibition efficiency of *m*-BTA is superior to that of BTA. The addition of Cl^- into the *m*-BTA-containing HEDP electrolyte can enhance the inhibition capability, even at a high anodic potential.

2) According to nano-scratch test, the thickness of the passive film formed in a HEDP electrolyte containing *m*-BTA and Cl^- is thicker than that formed in a HEDP electrolyte containing *m*-BTA alone.

3) The EDAX and XPS results demonstrate that the enhancement in the inhibition capability can be attributed to the incorporation of Cl^- into the *m*-BTA passive film and the formation of $[Cu(I)Cl(m\text{-BTA})]_n$ polymer film on Cu surface.

4) The polarization curves of Cu with or without abrasion in a HEDP electrolyte containing *m*-BTA and Cl^- prove that a suitable operating potential window from 1.0 to 1.7 V can be obtained. The ε_{ECMP} and Cu removal rate are greater than 0.95 and 600 nm/min, respectively. These results indicate that the addition of Cl^- into *m*-BTA-containing HEDP ECMP electrolyte is effective to increase the operating potential window, demonstrating a great potential for use in ECMP process.

References

[1] LIU F Q, DU T B, DUBOUST A, TSAI S, HSU W Y. Cu planarization in electrochemical mechanical planarization [J]. Journal of the Electrochemical Society, 2006, 153(6): C377−C381.

[2] OH Y J, PARK G S, CHUNG C H. Planarization of copper layer for damascene interconnection by electrochemical polishing in alkali-based solution [J]. Journal of the Electrochemical Society, 2006, 153(7): G617−G621.

[3] HUO J, SOLANKI R, MCANDREW J. Study of anodic layers and their effects on electropolishing of bulk and electroplated films of copper [J]. Journal of Applied Electrochemistry, 2004, 34(3): 305−314.

[4] LUO Q, BABU S V. Dishing effects during chemical-mechanical polishing of copper in acidic media [J]. Journal of the Electrochemical Society, 2000, 147(12): 4639−4644.

[5] CAI Chao, ZHANG Zhao, WEI Zhong-ling, YANG Jian-feng, LI Jin-feng. Electrochemical and corrosion behaviors of pure Mg in neutral 1.0% NaCl solution[J]. Transactions of Nonferrous Metals Society of China, 2012, 22(4): 970−976.

[6] STEWART K L, ZHANG J, LI S, CARTER P W, GEWIRTHA A A. Anion effects on Cu–benzotriazole film formation implications for CMP [J]. Journal of the Electrochemical Society, 2007, 154(1): D57−D63.

[7] BIGGIN M E, GEWIRTH A A. Infrared studies of benzotriazole on copper electrode surfaces: Role of chloride in promoting reversibility [J]. Journal of the Electrochemical Society, 2001, 148(5): C339−C347.

[8] LIN J Y, CHOU S W. Synergic effect of benzotriazole and chloride ion on Cu passivation in a phosphate electrochemical mechanical planarization electrolyte [J]. Electrochimica Acta, 2011, 56(9): 3303−3310.

[9] ZHAI W J, YANG Y Z. Tribo-electrochemical performance of copper ECMP in mixed phosphate electrolytes [J]. Advanced Materials Research, 2011, 314−316: 2565−2568.

[10] ZHAI W J, YANG Y Z. Screening test of phosphoric acid−bta slurries for copper ECMP based on inhibition efficiency [J]. Advanced Materials Research, 2011, 239−242: 920−923.

[11] TRIPATHI A, SUNI I I, LI Y Z, DONIAT F, McANDREW J. Cu

electrochemical mechanical planarization surface quality [J]. Journal of the Electrochemical Society, 2009, 156(7): H555−H560.
[12] KEAR G, BARKER B D, WALSH F C. Electrochemical corrosion of unalloyed copper in chloride media-a critical review [J]. Corrosion Science, 2004, 46: 109−135.
[13] SHATTUCK K G, LIN J Y, COJOCARU P, WEST A C. Characterization of phosphate electrolytes for use in Cu electrochemical mechanical planarization [J]. Electrochimica Acta, 2008, 53(28): 8211−8216.
[14] PADHI D, YAHALOM J, GANDIKOTA S, DIXIT G. Planarization of copper thin films by electropolishing in phosphoric acid for ULSI applications [J]. Journal of the Electrochemical Society, 2003, 150(1): G10−G14.
[15] TRIPATHI A, BURKHARD C, SUNI I I, LI Y Z, DONIAT F, BARAJAS A, McANDREW J. Electrolyte composition for Cu electrochemical mechanical planarization [J]. Journal of the Electrochemical Society, 2008, 155(11): H918−H922.
[16] BEHPOUR M, GHOREISHI S M, SOLTANI N, NIASARI M S. The inhibitive effect of some bis-N,S-bidentate Schiff bases on corrosion behaviour of 304 stainless steel in hydrochloric acid solution [J]. Corrosion Science, 2009, 51: 1073−1082.
[17] ALJOURANI J, RAEISSI K, GOLOZAR M A. Benzimidazole and its derivatives as corrosion inhibitors for mild steel in 1 M HCl solution [J]. Corrosion Science, 2009, 51(8): 1836−1843.
[18] SINGH A K, QURAISHI M A. Effect of 2,2 benzothiazolyl disulfide on the corrosion of mild steel in acid media [J]. Corrosion Science, 2009, 51(11): 2752−2760.
[19] ZHOU Wei, SONG Rong, JIANG Le-lun, XU Wen-ping, LIANG Guo-kai, CHENG De-cai, LIU Ling-jiao. Chemical etching process of copper electrode for bioelectrical impedance technology [J]. Transactions of Nonferrous Metals Society of China, 2012, 22(6): 1501−1506.
[20] FRIGNANI A, FONSATI M, MONTICELLI C, BRUNORO G. Influence of the alkyl chain on the protective effects of 1,2,3-benzotriazole towards copper corrosion. Part ii: formation and characterization of the protective films [J]. Corrosion Science, 1999, 41(6): 1217−1227.
[21] PAN C T, WU T T, LIU C F, SU C Y, WANG W J, HUANG J C. Study of scratching Mg-based BMG using nanoindenter with Berkovich probe [J]. Materials Science and Engineering A, 2010, 527(9): 2342−2349.
[22] CHAWLA S K, RICKETT B I, SANKARRAMAN N, PAYER J H. An X-ray photo-electron spectroscopic investigation of the air-formed film on copper [J]. Corrosion Science, 1992, 33(10): 1617−1631.
[23] DU T, VIJAYAKUMAR A, DESAI V. Effect of hydrogen peroxide on oxidation of copper in CMP slurries containing glycine and Cu ions [J]. Electrochimica Acta, 2004, 49(25): 4505−4512.

5-甲基苯并三氮唑作为电腐蚀抑制剂在铜电化学机械平坦化中的应用

边燕飞，翟文杰，朱宝全

哈尔滨工业大学 机电工程学院，哈尔滨 150001

摘　要：根据电化学分析，5-甲基苯并三氮唑(*m*-BTA)的腐蚀抑制能力要高于苯并三唑 (BTA)的。当羟基乙叉二膦酸(HEDP) 电解液中同时含有 *m*-BTA 及氯离子时，其抑制解离能力比只含有 *m*-BTA 的更好，即使施加更高的阳极氧化电位依然能保持良好的抑制能力。由电化学阻抗谱法、纳米划痕实验以及能谱分析结果得知，*m*-BTA 抑制能力的提升是因为整体钝化膜厚度的增加而引起的。由 X 射线光电子能谱分析得知，氯离子与 *m*-BTA 钝化层形成 $[Cu(I)Cl(m\text{-}BTA)]_n$ 高分子化合物，使得整体钝化层厚度增加。因此，在含有 *m*-BTA 的 HEDP 电解液中添加氯离子有助于 *m*-BTA 钝化层抑制能力的增强，进而更有效的电位操作区间得到扩展。

关键词：电化学机械平坦化；5-methyl-1H-benzotriazole；腐蚀抑制剂；氯离子

(Edited by Jing-hua FANG)